# Hypercomplex Quality Assessment of Multi/Hyperspectral Images

Andrea Garzelli, *Senior Member, IEEE*, and Filippo Nencini

***Abstract*—This letter presents a novel image quality index which extends the Universal Image Quality Index for monochrome images to multispectral and hyperspectral images through hypercomplex numbers. The proposed index is based on the computation of the hypercomplex correlation coefficient between the reference and tested images, which jointly measures spectral and spatial distortions. Experimental results, both from true and simulated images, are presented on spaceborne and airborne visible/infrared images. The results prove accurate measurements of inter- and intraband distortions even when anomalous pixel values are concentrated on few bands.**

***Index Terms*—Hypercomplex correlation coefficient (CC), hypercomplex number, image quality assessment, spectral distortion.**

## I. Introduction

IMAGE quality measurement is crucial for most image processing applications. The subjective or objective evaluation of the image quality can be carried out. Even if subjective judgment is very important, it is time consuming, laborious, and expensive, particularly when multiband images are considered. As a consequence, the objective evaluation is preferred to the subjective one.

Depending on the required information of the nondistorted images, objective quality assessment can be grouped into three classes: full reference (FR), reduced reference (RR), and no reference (NR) or blind. FR indexes require the availability of the nondistorted image. In RR methods, features extracted from both the nondistorted and distorted images are needed. When *a priori* knowledge of the distortion nature is available and can be easily exploited, NR indexes can be developed without any information of the reference original image.

Many FR quality indexes are based on the computation of errors between the reference and the distorted image, such as mean square error (mse), root mse, and peak signal-to-noise ratio. However, in many cases, these measurements may not match with the perceived visual quality [1]–[3]. Wang and Bovik [1] developed an image quality index referred as the Universal Image Quality Index (*UQI*). This index is based on the philosophy that structural information is extracted from the viewing field of the human eyes. As a consequence, a switch from error measurement to structural distortion measurement is carried out. The *UQI* index is composed by three factors: The first factor is the correlation coefficient (CC) between the images $x$ and $y$, the second one accounts for the mean bias and is always lower than or equal to one, and the third factor measures changes in contrast. The quality index *UQI* may be obtained by averaging the values computed on blocks, in order to account for spatial variability. The dynamic range of *UQI* is $[-1, 1]$, and the best value one is achieved if and only if the tested image is equal to the reference image for all pixels.

A lot of tested images have proven that the *UQI* index can be profitably used to assess the quality of distorted images [4]. However, this index has been developed to be applied to monochrome images, and to overcome this limitation, a weighted average of *UQI* indexes of color images can be carried out, as suggested in [5] and [6]. Furthermore, an improvement of UQI index (which is the Structural Similarity Image Index) has been introduced in [3] in order to mitigate possible numerical instabilities of statistical parameters.

In this letter, an image quality index, referred to as $Q2^n$, suitable to measure quality for multiband images having an arbitrary number of spectral bands, is proposed and applied to hyperspectral (HS) remote sensing images. The proposed quality index is a generalization of the *UQI* index for monoband images [1] and an extension of the $Q4$ index [7], which can be applied only to four-band images. The index assumes real values in the interval [0, 1], with 1 being the best value, which can be achieved if and only if the multiband image is identical to the reference image. The proposed index $Q2^n$ is derived from the theory of hypercomplex numbers, particularly of $2^n$-ons [8], [9]. The new index is made up of different factors to take into account for correlation, mean of each spectral band, intraband local variance, and the spectral angle. Thus, both intra- and interband (spectral) distortions are considered by a single index $Q2^n$. The index can be easily calculated, and it can be profitably applied to assess the quality of remote sensing HS images when a reference HS image is available.

This letter is organized into six sections. Sections II presents a general description of hypercomplex numbers. The main properties regarding the hypercomplex numbers and the evaluation of second-order statistics are described in Section III. Section IV introduces the novel index that is capable to measure the quality of multiband images. Several experiments have been carried out on HS images acquired by spaceborne and airborne spectral scanners. The typical causes of distortion are considered, as suggested in [10], and the effects of different pan-sharpening techniques are evaluated. Section V illustrates the data set used for the experiments and reports the experimental results which compare the proposed index with the state-of-the-art quality scores. Finally, Section VI draws the conclusions of this letter.

Manuscript received February 18, 2009; revised April 29, 2009. First published July 7, 2009; current version published October 14, 2009.

The authors are with the Department of Information Engineering, University of Siena, 53100 Siena, Italy (e-mail: garzelli@dii.unisi.it).

Color versions of one or more of the figures in this paper are available online at http://ieeexplore.ieee.org.

Digital Object Identifier 10.1109/LGRS.2009.2022650

## II. Review of Hypercomplex Numbers

Numbers are commonly thought of as a dense infinite set of things, including one and zero, that one may add, subtract, multiply, and (except for division by zero) divide. The real numbers and various subfields thereof, e.g., the rational, algebraic, and computable reals, are the prototypical example [9]. Reals can be considered as merely a 1-D subfield of the 2-D complex numbers. A new vision rose up with the introduction of the 4-D quaternions and the 8-D octonions—which continue the chain of inclusions begun by the complex numbers—and, in an entirely different direction, the surreals. The purpose of this section is to review the $2^n$-ons (pronunciation: "two-to-the-any-ons"), which is an infinite sequence of normed algebraic structures continuing the real $\subset$ complex $\subset$ quaternion $\subset$ octonion inclusion chain.

The $2^n$-ons were commonly previously thought incorrectly to be impossible. The $2^n$-ons can be defined recursively in terms of the $2^{n-1}$-ons. A $2^n$-on is a hypercomplex number that may be represented as

$$\mathbf{z} = z_0 + z_1 i_1 + z_2 i_2 + \cdots + z_{2^n-1} i_{2^n-1} \tag{1}$$

where $z_0, z_1, z_2, \ldots, z_{2^n-1}$ are real numbers, and $i_1, i_2, \ldots, i_{2^n-1}$ are hypercomplex unit vectors. Analogously to complex numbers, the conjugate $\mathbf{z}^*$ is given by

$$\mathbf{z}^* = z_0 - z_1 i_1 - z_2 i_2 - \cdots - z_{2^n-1} i_{2^n-1} \tag{2}$$

and the modulus by

$$|\mathbf{z}| = \sqrt{z_0^2 + z_1^2 + z_2^2 + \cdots z_{2^n-1}^2}. \tag{3}$$

## III. Evaluation of Hypercomplex CC Among Hypercomplex Numbers

In order to introduce the proposed index, we describe how to evaluate the hypercomplex CC among two hypercomplex numbers. In the next section, we will discuss how this result is the key to measure interband distortion.

Given two $2^n$-on hypercomplex random variables $\mathbf{z}$ and $\mathbf{v}$ represented in boldface, the hypercomplex covariance between $\mathbf{z}$ and $\mathbf{v}$ may be defined as

$$\operatorname{cov}(\mathbf{z}, \mathbf{v}) = E\left[(\mathbf{z} - \overline{\mathbf{z}})(\mathbf{v} - \overline{\mathbf{v}})\right] = E[\mathbf{z}\mathbf{v}^*] - \overline{\mathbf{z}} \cdot \overline{\mathbf{v}}^* = \sigma_{zv} \tag{4}$$

in which $\overline{\mathbf{z}} = E[\mathbf{z}]$ and $\overline{\mathbf{v}} = E[\mathbf{v}]$. In (4), the product of two hypercomplex numbers $\mathbf{z}$ and $\mathbf{v}^*$ has to be calculated to determine the hypercomplex covariance. Let us rewrite the $2^n$-on number $\mathbf{z}$ in the following form:

$$\begin{aligned}\mathbf{z} &= z_0 + i_1 \cdot z_1 + \cdots + i_{2^n-1} \cdot z_{2^n-1} \\ &= (z_0 + i_1 \cdot z_1 + \cdots + i_{2^{n-1}-1} \cdot z_{2^{n-1}-1}) \\ &\quad + i_{2^{n-1}}(z_{2^{n-1}} - i_1 \cdot z_{2^{n-1}+1} - i_{2^{n-1}-1} \cdot z_{2^n-1}) \\ &= \mathbf{a} + i_{2^{n-1}} \cdot \mathbf{b}\end{aligned} \tag{5}$$

where the following properties apply:

$$i_{2^{n-1}} \cdot i_l = -i_{2^{n-1}+l}, \qquad 1 \le l \le 2^{n-1} - 1 \tag{6}$$

and in the same way for the $\mathbf{v}$ hypercomplex number

$$\begin{aligned}\mathbf{v}^* &= v_0 - i_1 \cdot v_1 - \cdots - i_{2^n-1} \cdot v_{2^n-1} \\ &= (v_0 - i_1 \cdot z_1 - \cdots - i_{2^{n-1}-1} \cdot z_{2^{n-1}-1}) \\ &\quad + i_{2^{n-1}} \cdot (-v_{2^{n-1}} + i_1 \cdot v_{2^{n-1}+1} + i_{2^{n-1}-1} \cdot v_{2^n-1}) \\ &= \mathbf{c} + i_{2^{n-1}} \cdot \mathbf{d}.\end{aligned} \tag{7}$$

The Cayley–Dickson property [8] is used to produce a sequence of algebras over the field of real numbers, each with twice the dimension of the previous one. This property is used to calculate the product of two $2^n$-on numbers

$$\begin{aligned}\mathbf{z} \cdot \mathbf{v}^* &= (\mathbf{a} + i_{2^{n-1}} \cdot \mathbf{b}) \cdot (\mathbf{c} + i_{2^{n-1}} \cdot \mathbf{d}) \\ &= (\mathbf{a}, \mathbf{b}) \cdot (\mathbf{c}, \mathbf{d}) \\ &= (\mathbf{a} \cdot \mathbf{c} - \mathbf{d} \cdot \mathbf{b}^*, \mathbf{a}^* \cdot \mathbf{d} + \mathbf{c} \cdot \mathbf{b}) \\ &= (\mathbf{a} \cdot \mathbf{c} - \mathbf{d} \cdot \mathbf{b}^*) + i_{2^{n-1}}(\mathbf{a}^* \cdot \mathbf{d} + \mathbf{c} \cdot \mathbf{b}).\end{aligned} \tag{8}$$

The $\mathbf{z} \cdot \mathbf{v}^*$ product is given by the combination of four terms $\mathbf{a} \cdot \mathbf{c}$, $\mathbf{d} \cdot \mathbf{b}^*$, $\mathbf{a}^* \cdot \mathbf{d}$, and $\mathbf{c} \cdot \mathbf{b}$, each of which is determined by the product of two hypercomplex numbers with a dimension reduced by two, i.e., with $2^{n-1}$ dimensionality. This suggests that (8) can be applied iteratively until a simple product among complex numbers is given.

Starting from (4), the hypercomplex CC between two $2^n$-on random variables may be defined as the normalized covariance

$$\varrho(\mathbf{z}, \mathbf{v}) = \frac{\sigma_{zv}}{\sigma_z \sigma_v} \tag{9}$$

in which $\sigma_z$ and $\sigma_v$ are the square roots of the variances of $z$ and $v$ and are obtained by

$$\sigma_{\mathbf{z}} = E\left[|\mathbf{z}|^2\right] - |\overline{\mathbf{z}}|^2 \tag{10}$$

$$\sigma_{\mathbf{v}} = E\left[|\mathbf{v}|^2\right] - |\overline{\mathbf{v}}|^2. \tag{11}$$

## IV. New Image Quality Index $Q2^n$

The proposed quality index is a generalization of the *UQI* index defined in [1] for an original image signal $z$ and a test image signal $v$, which can be stated as

$$Q_{N\times N} = \frac{\sigma_{z,v}}{\sigma_z \sigma_v} \cdot \frac{2\bar{z}\bar{v}}{(\bar{z})^2 + (\bar{v})^2} \cdot \frac{2\sigma_z \sigma_v}{\sigma_z^2 + \sigma_v^2} \tag{12}$$

where $\sigma_f$ denotes the standard deviation of $f$, and $\sigma_{z,v}$ is the cross-covariance of $z$ and $v$, all computed over a given $N \times N$ block. In practice, the first factor is the CC, the second one (always $< 1$ and $= 1$ if and only if $z = v$) accounts the changes of the mean bias; analogously, the third one measures the change in contrast. Eventually, the *UQI* index is obtained by averaging the values obtained starting from all the $N \times N$ blocks of the images $z$ and $v$. This quality factor can be applied only to monochrome images.

As an extension of the $Q4$ index proposed in [7], the novel index $Q2^n$ assumes a real value in the interval [0, 1] with 1 being the best value. The correlation, the mean of each spectral band, and the intraband local variance are also taken into account by *UQI* for each band, as shown in (12), while the spectral angle is introduced by $Q2^n$ by the modulus of

hypercomplex CC of multivariate data [7] in order to measure the alignment of spectral vectors [11]. In this way, both spatial and spectral distortions are considered by a single parameter. $Q2^n$ can be computed from

$$\mathbf{Q2^n_{N\times N}} = \frac{\sigma_{\mathbf{z},\mathbf{v}}}{\sigma_{\mathbf{z}}\sigma_{\mathbf{v}}} \cdot \frac{2\bar{\mathbf{z}}\bar{\mathbf{v}}}{(\bar{\mathbf{z}})^2 + (\bar{\mathbf{v}})^2} \cdot \frac{2\sigma_{\mathbf{z}}\sigma_{\mathbf{v}}}{\sigma_{\mathbf{z}}^2 + \sigma_{\mathbf{v}}^2} \tag{13}$$

where the product of $\mathbf{z}$ by the hypercomplex conjugate of $\mathbf{v}$, namely $\mathbf{v}^*$, has to be intended as a product of $2^n$-ons. The value of $2^n$-on obtained by HS CC is calculated by (4), (8), and (9).

Finally, $Q2^n$ is obtained by averaging the magnitudes of all $\mathbf{Q2^n_{N\times N}}$ over the whole image, i.e.,

$$Q2^n = E\left[|\mathbf{Q2^n_{N\times N}}|\right]. \tag{14}$$

The more $Q2^n$ approaches to unity, the higher becomes the radiometric and spectral quality of the fused image.

If the number of bands is not a power of two, the problem can be similarly considered by appropriately zero-padding the image bands to analyze the overall data with $2^n$ spectral bands. The null bands do not influence the image quality measurement. Moreover, the value taken by $Q2^n$ is *invariant* with respect to the order of assignment of the multiband hypercomplex components, even though the commutative property is not verified for a $2^n$-on.

## V. Experimental Results

The proposed quality index has been assessed on two image data sets acquired by the Hyperion spaceborne HS scanner and by the Airborne Visible/Infrared Imaging Spectrometer (AVIRIS) airborne HS scanner, respectively. The 242 HS bands of Hyperion sensor (at 30-m spatial resolution) span from 0.35 to 2.6 $\mu$m, while the AVIRIS data set is characterized by 224 contiguous spectral channels with wavelengths from 0.4 to 2.5 $\mu$m. The Hyperion data set has been used for evaluating the effects of different pan-sharpening techniques through a co-registered panchromatic band acquired by the Advanced Land Imager (ALI) sensor (at 10-m spatial resolution). The quality of the AVIRIS data set has been assessed after JPEG-2000 compression (JPK2), Gaussian spectral filtering (SF) [10], and degradation by additive white Gaussian noise (AWGN).

In the Hyperion experiment, we have investigated the effects of pan sharpening of Hyperion image data by means of an ALI panchromatic band (3 : 1 spatial scale ratio). Fusion algorithm performances are typically evaluated in terms of radiometric and spectral distortions when compared with the reference HS bands. However, the reference HS bands are not available, and to overcome this problem, the data sets have been spatially degraded by a factor of three (the scale ratio between HS and panchromatic acquisitions), according to the protocol proposed in [12]. Therefore, image quality indexes have been calculated between fused images obtained from spatially degraded data and the original HS data. Three fusion methods were applied to the considered data set: the generalized intensity–hue–saturation (GIHS) method [13], the Gram–Schmidt (GS) spectral sharpening method [14], and the modified high-pass filtering method [15] with a filter characterized by a 1/3 cutoff frequency (HPF3). An average single-band (SB) CC has been calculated to evaluate the geometric distortion between fused multispectral products and true reference HS originals. For spectral distortion, spectral angle mapper (SAM) is compared throughout. To this purpose, the data set has been spatially degraded by three, according to the protocol proposed in [12], and statistics have been calculated between the fused and original data. Accordingly to $Q4$ [7], $Q2^n$ is calculated on 32 $\times$ 32 blocks and then averaged as in (14).

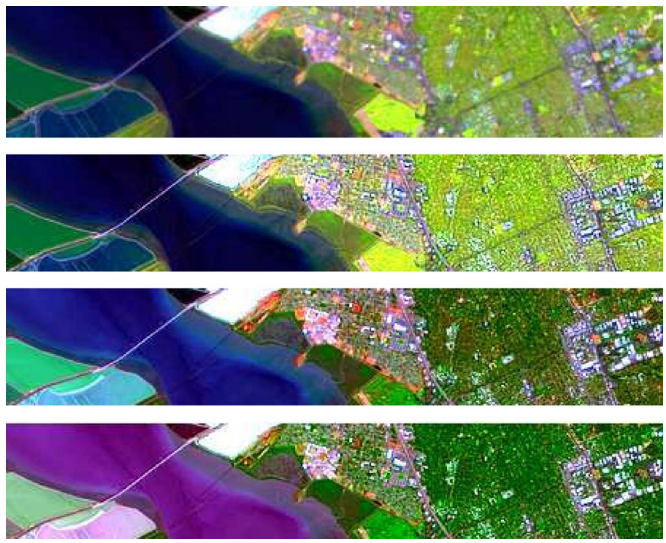

Fig. 1. Color composites of 80 $\times$ 450 details of Hyperion data. (From top to bottom) Reference 30-m HS image, HPF3, GS, and GIHS.

TABLE I
Results for Pan-Sharpened Hyperion Data

| | $Q2^n$ | $Q_{avg}$ | $CC_{avg}$ | $SAM$ |
|---|---|---|---|---|
| Original | 1 | 1 | 1 | 0 |
| HPF3 | 0.835 | 0.857 | 0.966 | 2.485 |
| GS | 0.599 | 0.525 | 0.750 | 9.694 |
| GIHS | 0.547 | 0.542 | 0.681 | 8.467 |

Fig. 1 shows the reference and fused images for the tested methods in the following band combination: blue—band 17 (518.39 nm), green—band 47 (823.65 nm), and red—band 149 (1638.81 nm). Visual results highlight that the HPF3 algorithm better preserves spectral information after spatial enhancement, while the other algorithms, like GIHS and GS, are specifically designed for spatial preservation, but they fail in terms of spectral preservation.

Average $Q$ and CC from SB values

$$Q_{\text{avg}} = \frac{1}{N}\sum_{i=1}^{N} Q_i \qquad CC_{\text{avg}} = \frac{1}{N}\sum_{i=1}^{N} CC_i \tag{15}$$

have been calculated to evaluate distortions between fused HS products and true reference HS originals. For spectral distortion, SAM [16] is compared throughout. The results of $Q2^n$ in Table I confirm the visual results of Fig. 1 and are in accordance with the average SB indexes.

Table II presents the results of other experiments performed on AVIRIS data, specifically a 256 $\times$ 256 detail on bands 1 $\div$ 224 of the Indian Pine acquisition (August 20, 1992).

TABLE II
RESULTS FOR JPEG-2000 COMPRESSED AND SPECTRALLY FILTERED AVIRIS DATA

| | | $Q2^n$ | $Q_{avg}$ | $CC_{avg}$ | $SAM$ |
|---|---|---|---|---|---|
| | Original | 1 | 1 | 1 | 0 |
| JP2K | CR=10 | 0.879 | 0.922 | 0.901 | 0.945 |
| | CR=30 | 0.746 | 0.817 | 0.868 | 2.247 |
| SF | L=3 | 0.335 | 0.913 | 0.978 | 5.845 |
| | L=5 | 0.081 | 0.849 | 0.965 | 9.284 |

TABLE III
RESULTS ON AVIRIS DATA AFFECTED BY AWGN

| | $Q2^n$ | $Q_{avg}$ | $Q_g$ | $Q_{min}$ | $CC_{avg}$ | $SAM$ |
|---|---|---|---|---|---|---|
| REF | 1 | 1 | 1 | 1 | 1 | 0 |
| UD | 0.843 | 0.845 | 0.844 | 0.761 | 0.936 | 0.610 |
| SB | 0.845 | 0.996 | 0.986 | 0.044 | 0.997 | 0.155 |

Concerning JPK2, it results that $CC_{\rm avg}$ is much less sensitive than the other indexes to capture the significant quality difference between data obtained with low $(CR = 10)$ or high $(CR = 30)$ compression ratios. In the case of SF by a rectangular filter with $L$ coefficients, $Q2^n$ only is capable to clearly catch any distortion in the spectral dimension, even for a very short smoothing filter $(L = 3)$. In fact, average quality indexes, except SAM to some extent, are not able to detect few highly distorted bands, i.e., those bands in this experiment which are located along the spectral dimension near signal-to-noise-ratio transitions from high to low values.

Moreover, an average of SB indexes fails to measure spectral distortion when errors among reference and test images are concentrated on a limited subset of bands.

To prove that, as a further analysis, we evaluated the quality of AVIRIS data affected by a simulated AWGN. Table III shows the results obtained on images with noise uniformly distributed (UD) on all bands and concentrated on an SB, given the same amount of noise power. The proposed index has been compared with the average SB indexes, and the geometric mean

$$Q_g = \sqrt[N]{\prod_{i=1}^{N} Q_i} \tag{16}$$

where $Q_i = 0$ if $Q_i < 0$, and the minimum value of $Q_i$, referred to as $Q_{\rm min}$, is considered in order to give evidence to the most distorted band. The average SB indexes $Q_{\rm avg}$ and $Q_g$ are not suitable to measure SB distortion, as confirmed by the numerical values which are sensibly greater than the corresponding UD values and very close to one. $CC_{\rm avg}$ and SAM are not able to measure AWGN distortion, regardless of noise distribution across bands: $SAM \approx 0$ and $CC_{\rm avg} \approx 1$ in both SB and UD cases. On the other hand, $Q_{\rm min}$ is too much sensitive to SB distortion, while it is not sufficiently sensitive to distortion due to UD noise. Conversely, $Q2^n$ values are lower than one and almost invariant in both cases, which is correct, since the noise power is constant for the SB and UD cases. $Q_{\rm min}$ should be evaluated together with $Q_{\rm avg}$ or $Q_g$ to give evidence to both UD and band-concentrated distortions. As a consequence, a straightforward ranking of distorted multiband images is not possible by using a single quality index selected among the following: $Q_{\rm min}$, $Q_{\rm avg}$, $Q_g$, $\rm CC_{avg}$, and SAM. This limitation can be successfully overcome by the proposed $Q2^n$ index.

## VI. CONCLUSION

The proposed $Q2^n$ index has been proven to be very useful for FR quality assessment of multiband images. Hypercomplex numbers are used to achieve a unique normalized score index capable to measure the fidelity of a multiband image with respect to a known reference in terms of spatial and spectral distortions. A hypercomplex CC is calculated exploiting the Cayley–Dickson property, and the result is used in a generalized expression of the *UQI* index [1] in order to measure both spatial and spectral distortions.

The experimental results obtained on two HS image data sets have demonstrated that the proposed index is capable to assess the image quality in a more complete and efficient way than average- or minimum-based state-of-the-art image quality indexes.

## REFERENCES


[1] Z. Wang and A. C. Bovik, "A universal image quality index," *IEEE Signal Process. Lett.*, vol. 9, no. 3, pp. 81–84, Mar. 2002.

[2] Z. Wang, A. C. Bovik, and L. Lu, "Why is image quality assessment so difficult?" in *Proc. IEEE Int. Conf. Acoust., Speech, Signal Process.*, May 2002, vol. 4, pp. 3313–3316.

[3] Z. Wang, A. C. Bovik, H. R. Sheikh, and E. P. Simoncelli, "Image quality assessment: From error visibility to structural similarity," *IEEE Trans. Image Process.*, vol. 13, no. 4, pp. 600–612, Apr. 2004.

[4] H. R. Sheikh, M. F. Sabir, and A. C. Bovik, "A statistical evaluation of recent full reference image quality assessment algorithms," *IEEE Trans. Image Process.*, vol. 15, no. 11, pp. 3440–3451, Nov. 2006.

[5] Z. Wang, L. Lu, and A. C. Bovik, "Video quality assessment based on structural distortion measurement," *Signal Process.: Image Commun.*, vol. 19, no. 2, pp. 121–132, Feb. 2004.

[6] A. Medda and V. DeBrunner, "Color image quality index based on the UIQI," in *Proc. IEEE Southwest Symp. Image Anal. Interpretation*, 2006, pp. 213–217.

[7] L. Alparone, S. Baronti, A. Garzelli, and F. Nencini, "A global quality measurement of pan-sharpened multispectral imagery," *IEEE Geosci. Remote Sens. Lett.*, vol. 1, no. 4, pp. 313–317, Oct. 2004.

[8] W. D. Smith, *Quaternions, octonions, and now, 16-ons and 2 n-ons; New kinds of numbers*, 2004. [Online]. Available: http://www.math.temple.edu/~wds/homepage/nce2.pdf

[9] H. B. Ebbinghaus, *Numbers*. New York: Springer-Verlag, 1991.

[10] E. Christophe, D. Leger, and C. Mailhes, "Quality criteria benchmark for hyperspectral imagery," *IEEE Trans. Geosci. Remote Sens.*, vol. 43, no. 9, pp. 2103–2114, Sep. 2005.

[11] R. Touzi, A. Lopes, J. Bruniquel, and P. W. Vachon, "Coherence estimation for SAR imagery," *IEEE Trans. Geosci. Remote Sens.*, vol. 37, no. 1, pp. 135–149, Jan. 1999.

[12] L. Wald, T. Ranchin, and M. Mangolini, "Fusion of satellite images of different spatial resolutions: Assessing the quality of resulting images," *Photogramm. Eng. Remote Sens.*, vol. 63, no. 6, pp. 691–699, 1997.

[13] T. M. Tu, S. C. Su, H. C. Shyu, and P. S. Huang, "A new look at IHS-like image fusion methods," *Inf. Fusion*, vol. 2, no. 3, pp. 177–186, Sep. 2001.

[14] C. A. Laben and B. V. Brower, "Process for enhancing the spatial resolution of multispectral imagery using pan-sharpening," U.S. Patent 6 011 875, Jan. 4, 2000.

[15] P. S. Chavez, S. C. Sides, and J. A. Anderson, "Comparison of three different methods to merge multiresolution and multispectral data: Landsat TM and SPOT panchromatic," *Photogramm. Eng. Remote Sens.*, vol. 57, no. 3, pp. 295–303, Mar. 1991.

[16] L. Alparone, B. Aiazzi, S. Baronti, and A. Garzelli, "Sharpening of very high resolution images with spectral distortion minimization," in *Proc. IEEE IGARSS*, 2003, vol. 1, pp. 458–460.